

An Energy-Based Analysis of the Feijão Tailings Dam Failure

Kaitlyn O’Sullivan, Western University, Canada

Abouzar Sadrekarimi, Western University, Canada

Abstract

In 2019 the Feijão tailings dams in Brazil failed catastrophically, killing 270 people, and adding to the environmental devastation from the Fundão failure three years earlier. Both the Fundão and the Feijão failures have since been attributed to a phenomenon called static liquefaction; a very common, but poorly understood, facet of soil mechanics. The methods used to determine this cause of failure were through cone penetration correlations and state parameter analysis. This paper examines a different method of static liquefaction analysis – the energy method. Energy analysis has been used for cyclic liquefaction assessment by some researchers, but has not yet been applied to static liquefaction.

Based on triaxial testing data on tailings from the Feijão dam, the energy capacity (E_c) of the tailings was determined and correlated to void ratio. Then, using the finite element program RS2 from Rocscience, the work imposed by gravitational stress (E_a) was calculated. The ratio between E_c and E_a was then determined, where the soil would be prone to liquefaction if the ratio was less than one. Further analyses were then conducted where the liquefied shear strength of the tailings was assigned to those sections where the ratio between E_c and E_a was less than one. The progressive nature of static liquefaction was considered by repeating the finite element analysis until no more saturated layers underwent liquefaction. This method was able to accurately predict failure of the tailings mass, as well as find a critical slip surface that was consistent with field observations.

Introduction

Liquefaction is a complex topic in soil mechanics. While static liquefaction has been observed for several decades (Silvis and de Groot, 1995), it was not until the Fundão and the Feijão tailings dam failures in Brazil a few years ago that interest in static liquefaction was greatly renewed (Morgenstern et al., 2016; Robertson et al., 2019). There are many different definitions of liquefaction and a multitude of types. For the purposes of this paper, the simple definition from Jefferies and Been (2016) will be used: “Soil liquefaction is a phenomenon in which soil loses much of its strength or stiffness for a generally short time

but nevertheless long enough for liquefaction to be the cause of many failures, deaths, and major financial losses.” They define two main types of liquefaction: static liquefaction (caused by monotonic loading), and cyclic-induced liquefaction (caused by cyclic loading).

Over the years there have been many methods put forth for assessing a soil’s susceptibility to liquefaction and how to apply it in stability analyses. For static liquefaction, undrained liquefaction triggering, $s_u(\text{yield})$, and post-liquefaction, $s_u(\text{liq})$, strengths are found from q_{c1} , (corrected cone tip resistance from CPT), which are then used in stability analyses to determine the triggering of static liquefaction and whether a flow failure could occur (Sadrekarimi, 2016, 2020). The main drawbacks of these empirical methods are two-fold: first, the CPT correlations relate all soils to an “equivalent clean sand resistance”, which is poorly defined and understood (Jefferies and Been, 2016). Second, these do not account for the displacements induced in the soil and are stress-path dependent.

Some researchers have applied a different approach to the assessment of cyclic liquefaction – the energy method (Liang, 1995; Dief, 2000; Green, 2001; Kokusho, 2013). The main advantage of using energy for cyclic loading is that energy is a scalar parameter that is independent of the number of loading cycles. Liang (1995) proposed the following procedure for determining liquefaction susceptibility of a soil under cyclic loading:

1. The energy dissipated per unit volume (the energy capacity) is calculated by finding the area of the hysteretic loops. This is plotted against depth.
2. The amount of energy dissipated during the cyclic loading is then calculated and plotted with depth.
3. If the energy calculated in step 1 is less than that calculated in step 2, cyclic liquefaction could occur.

This method has only been applied to cyclic liquefaction. This paper examines the application of the energy method to static liquefaction.

Methodology

Energy capacity

The first step of the energy method is to find the energy capacity of the soil up to the point of instability, as demonstrated in Figure 1. As shown in this figure, instability is defined as the point of maximum deviator stress in an undrained monotonic shear test (Lade, 1992) after which a loose soil undergoes strain softening and strength reduction during undrained loading. e_c and σ'_c show the consolidation void ratio and confining pressure prior to shearing, respectively.

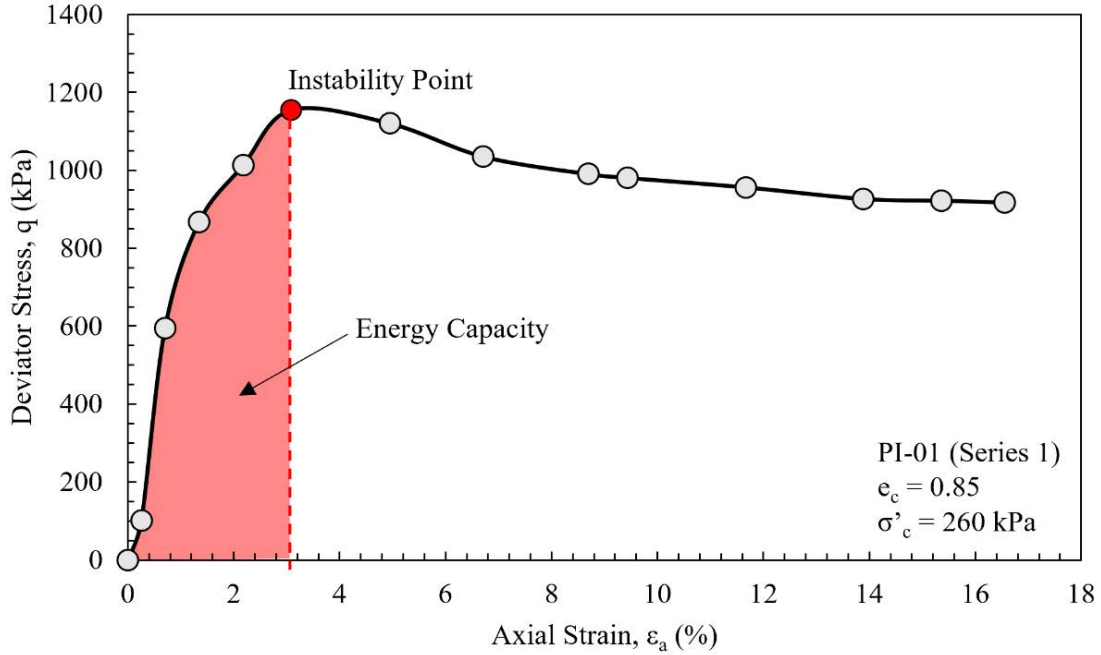


Figure 1: Energy capacity and instability point for a coarse tailings sample from the Feijão dam in an undrained triaxial compression test (Robertson et al., 2019)

In cyclic loading, the energy capacity is the area of the hysteretic loops (Liang, 1995). In monotonic loading, however, there are no loops where area can be calculated; instead, there is a single curve in a stress-strain diagram. Energy capacity per unit volume (E_c) is thus found by integrating the stress-strain curve using the trapezoidal rule as below:

$$E_c = \frac{1}{2} \sum_{i=1}^{n-1} (q_{i+1} + q_i) (\epsilon_{a,i+1} - \epsilon_{a,i}) \quad (\text{eq. 1})$$

Where n is the total number of increments, q_i is the i^{th} increment of deviatoric stress, and $\epsilon_{a,i}$ is the i^{th} increment of axial strain. The triggering E_c is found by calculating Equation 1 up to the point of instability i.e., peak deviator stress.

Finite element model

A finite element model (FEM) of the Feijão dam was created, as shown in Figure 2. For this analysis, the program RS2 from Rocscience was used as it allows users to define their own equations in the interpretation stage of the analysis. This allowed energy values to be extracted and visualized.

A plane strain model was setup for the critical section of the Feijão dam (Section 3'-3'). To model failure, the shear strength reduction (SSR) method was implemented. SSR is equivalent to determining a factor of safety (FoS) using limit equilibrium methods (Griffiths and Lane, 1999). In the SSR analysis, the shear strength of the chosen materials was reduced by a certain factor until failure occurred. This factor is called the strength reduction factor (SRF). The model was built over 14 stages, mirroring the actual construction stages of the dam (Robertson et al., 2019). Each stage consisted of a dam raise, tailings deposition, and water table change. The final stage of the model is shown in Figure 2. The numbers in brackets beside the dams indicate the stages of dam raising from Robertson et al. (2019).

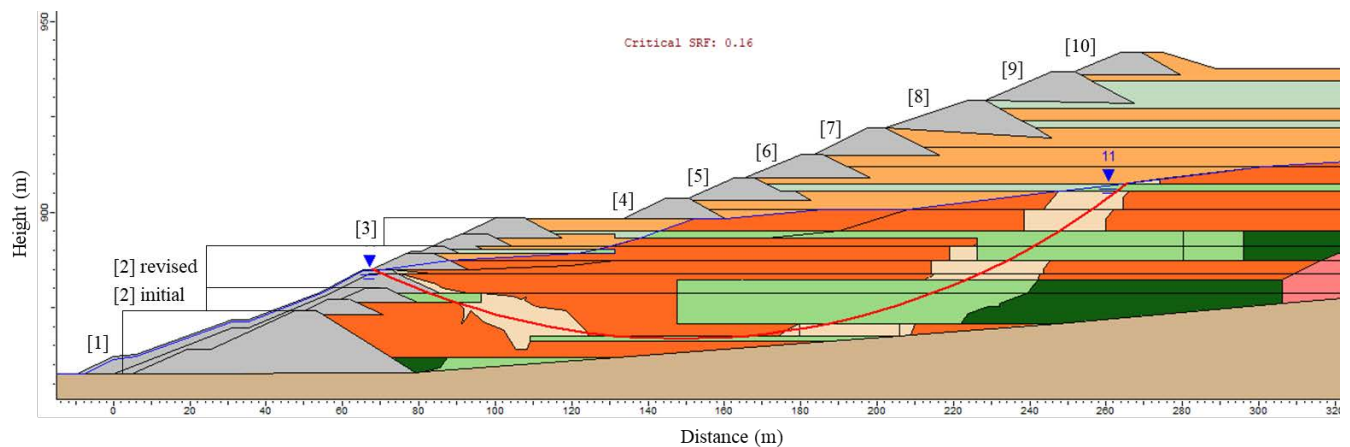





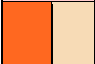
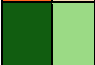
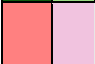


Figure 2: Final iteration for the finite element model of the Feijão dam used in this study

Mohr-coulomb strength parameters were used for all drained materials in Table 1. More advanced constitutive models, such as those that consider softening/hardening behaviour, could not be used due to limitations of the SSR analysis in RS2. Presently, it is not possible to determine closed-form relationships for material models with nonlinear criteria. Some approximations for material models like the Generalized Hoek-Brown model have been developed, but none have been created for the softening-hardening material models. Since Mohr-Coulomb parameters were readily available from the expert report, those were selected. Drained parameters for the tailings were used for all stages except in the final stage of analysis where the tailings behaviour was switched to undrained parameters.

Latter iterations would then use the post-liquefaction strength parameters for the respective zones. Table 1 summarizes the parameters used in these analyses. In this table, γ is the unit weight of the material, n is the porosity, E is the Young's modulus, ϕ is the friction angle, c' is cohesive strength, $s_u(\text{yield})/\sigma'_v$ is the triggering strength ratio, and $s_u(\text{liq})/\sigma'_v$ is the post-liquefaction strength ratio.

Table 1: Model parameters used in the analyses of this study

Material	Colour in model	γ	n	E	ϕ	c'	$s_u(\text{yield})/\sigma'_v$	$s_u(\text{liq})/\sigma'_v$
		(kN/m ³)		(MPa)	(°)	(kPa)		
Foundation		22	0.31	550	30	40	–	–
Berm		22	0.30	50	36	0	–	–
Coarse tailings (drained)		22	0.50	35	38	0	–	–
Loose tailings (drained)		22	0.59	7.5	36	0	–	–
Slimes (drained)		20	0.49	7.5	33	0	–	–
Coarse tailings (yield/liq)		22	0.50	14.5			0.37	0.01
Loose tailings (yield/liq)		22	0.59	5.5			0.37	0.01
Slimes (yield/liq)		20	0.49	5.5			0.37	0.01

The work imposed by gravitational stresses in the model (E_a) was calculated using Equation 2, derived for plane strain conditions (i.e., no shear stress or strain in the out-of-plane dimension) as below:

$$E_a = \sigma'_{xx}\varepsilon_{xx} + \sigma'_{yy}\varepsilon_{yy} + 2\tau_{xy}\gamma_{xy} \quad (2)$$

Void ratios (e_c) of the tailings were also calculated in the model based on their variation with depth deduced from the expert report (Robertson et al., 2019). Energy capacity was then determined using the relationship between E_c and e_c established through the data analysis discussed later in Figure 4. The tailings mass above the slip surface was split into sections, then the ratio between E_c and E_a was calculated. If the section had $E_c/E_a < 1$ then it was assumed to liquefy, for which the post-liquefaction strength ratios of Table 1 were assigned.

To account for the progressive nature of liquefaction, multiple iterations of the model were run, exemplified by Figure 3. First, the triggering analysis was carried out where the soil beneath the water table was assigned $s_u(\text{yield})$. From this analysis, areas where $E_c < E_a$ were identified. In the subsequent analysis, those areas were assigned $s_u(\text{liq})$. Additional areas where $E_c < E_a$ were found and then assigned $s_u(\text{liq})$. This process continued until there were no more areas that underwent static liquefaction (i.e., $E_c < E_a$).

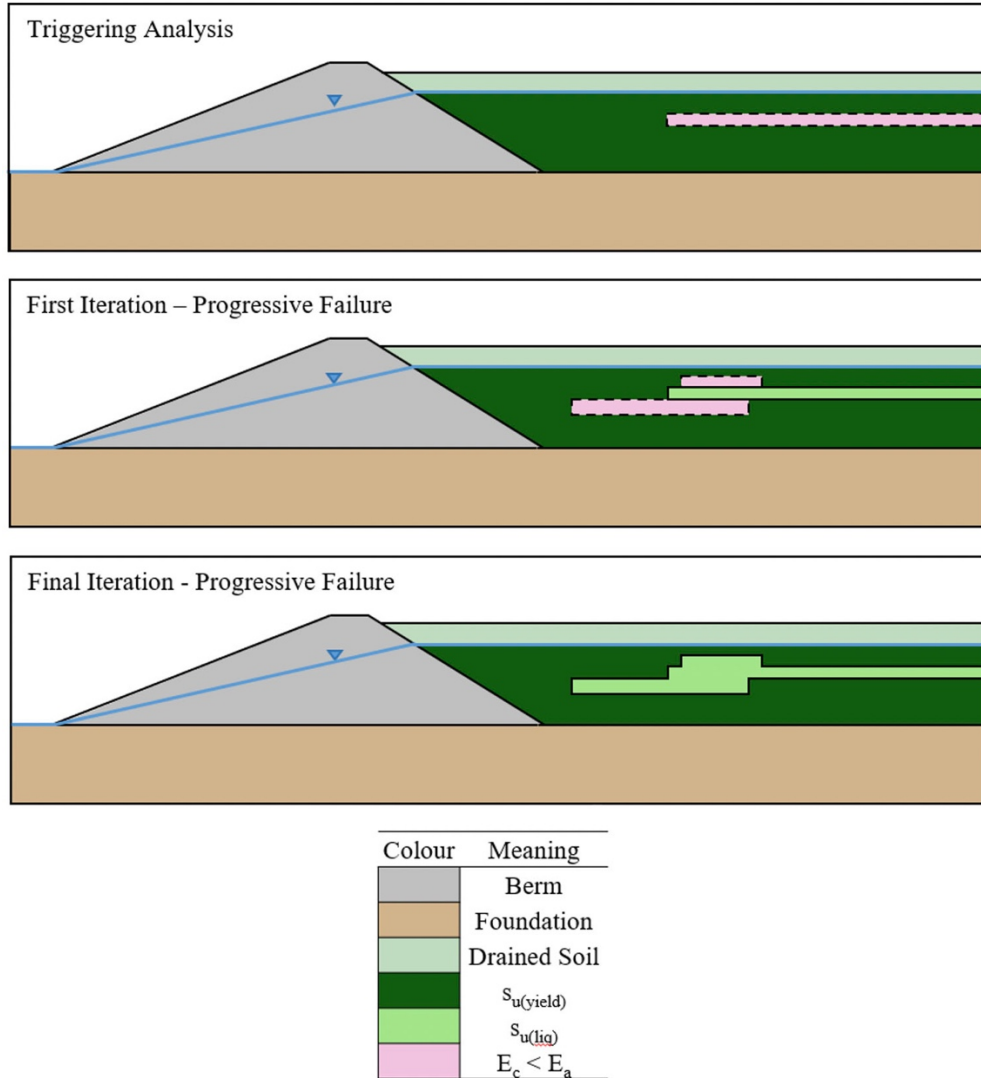


Figure 3: Example of progressive failure analysis

In addition to the FEM, limit equilibrium analyses (LEM) were also carried out using Slide2 to mirror those created in RS2. Limit equilibrium models were made to compare the differences in the slip surface and factor of safety determined from the LEM and FEM analyses.

Results and discussion

The energy capacities of coarse and fine tailings for the Feijão dam are shown in Figure 4 in relation to their e_c . The triaxial data available for the fine tailings were from two investigations in 2016 and 2019, with the 2019 investigation being after the failure (Robertson et al., 2019). The data for the coarse tailings were only from 2016, prior to failure. The 2019 data points were from undrained triaxial tests on anisotropically-consolidated specimens, while data from 2016 were based on undrained triaxial tests on specimens

subjected to isotropic consolidation. The anisotropic data were included to obtain energy estimates for fines tailings with high e_c . Nevertheless, the same $E_c - e_c$ relationship was found from both the isotropically- and the anisotropically-consolidated specimens of fine tailings. The effect of void ratio was more significant on the fine tailings than for the coarse tailings. Though for both tailings E_c decreased non-linearly with increasing e_c , the coarse tailings presented higher E_c than the fine tailings for the same e_c , with the difference diminishing at $e_c < 0.85$.

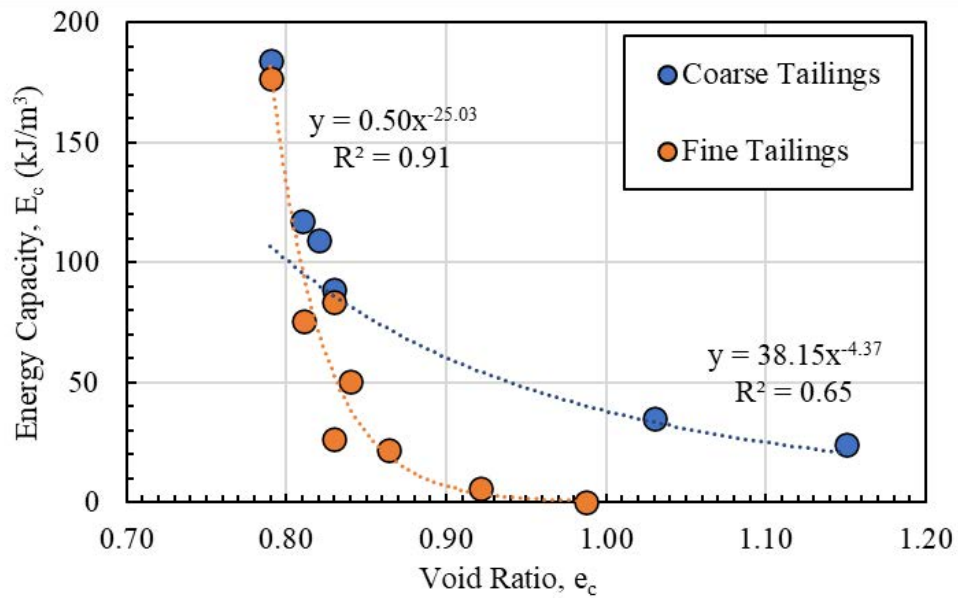


Figure 4: Relationships between energy capacity and void ratio for Feijão tailings

Using E_c values from Figure 4, Table 2 summarizes the FoS and SRF found from the LEM and FEM analyses. Note that in this table $s_u(\text{yield})$ was assigned to all tailings zones under the water table in the triggering analysis, whereas $s_u(\text{liq})$ was assigned to the same zones in the post-liquefaction analysis. For the progressive failure analysis, $s_u(\text{liq})$ was assigned to tailings undergoing liquefaction as determined based on their energy capacities ($E_c/E_a < 1$).

Table 2: Comparison of FoS and SRF from the analyses of this study

Model type	SRF (FEM)	FoS (LEM)
Triggering	1.24	1.08
Post-liquefaction	0.14	0.21
Progressive failure	0.16	0.45

As expected, the lowest FoS and SRF were found for the post-liquefaction model with a relatively higher FoS than SRF. However, FoS (= 0.45) and SRF (= 0.16) for the progressive failure model presented a larger difference, likely because of the additional iterations conducted in a progressive failure type analysis which amplified the underlying differences between the two analysis methods. In fact, the SRF from the post-liquefaction and progressive failure analyses were very similar (0.14 and 0.16). Despite the lower SRF in the post-liquefaction and progressive failure analyses than FoS, a higher SRF = 1.24 was obtained in the liquefaction triggering analysis compared to FoS = 1.08. This was because of the differences in the energy based and force equilibrium-based methods used to determine the triggering of static liquefaction in the FEM and the LEM methods, respectively.

Table 3 further summarizes the factors of safety and strength reduction factors for each iteration of the progressive failure analysis. As shown in this table, both FoS and SRF rapidly dropped following the triggering of liquefaction in the fine tailings in iteration 1. Iteration 2 is when some of the coarse tailings liquefy, which further drops FoS and SRF values to respectively 0.54 and 0.34. Iteration 3 sees a larger part of the coarse tailings liquefy along the slip surface. After this iteration, only small areas liquefy, and an equilibrium is reached where FoS and SRF tend to stabilize in iterations 4 and 5.

Table 3: Changes in factor of safety throughout progressive failure analysis

Iteration	SRF (RS2)	FoS (Slide2)
Triggering analysis	1.24	1.08
1	0.73	0.82
2	0.34	0.54
3	0.20	0.44
4	0.16	0.46
5	0.16	0.45

Despite the differences in SRF and FoS, similar slip surfaces were developed in these analyses for each case, as shown in Figure 5-8. Figures 5 and 6 show the slip surfaces from FEM (RS2) and LEM (Slide2) analyses respectively where all tailings below the water table liquefy. Figures 7 and 8 further show the critical slip surfaces from RS2 and Slide2 determined based on energy and force equilibrium progressive failure analyses, respectively.

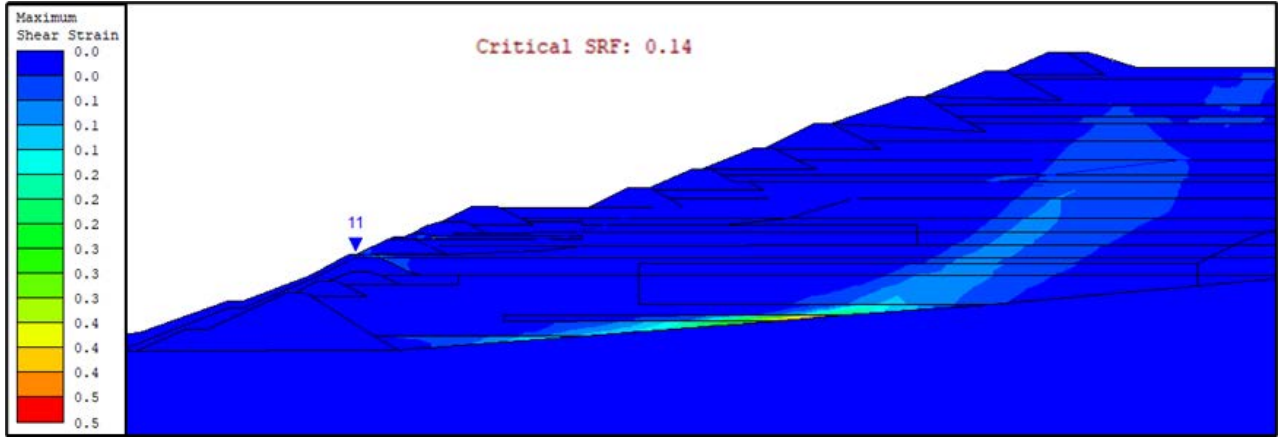


Figure 5: Slip surface from RS2 for post-liquefaction analysis

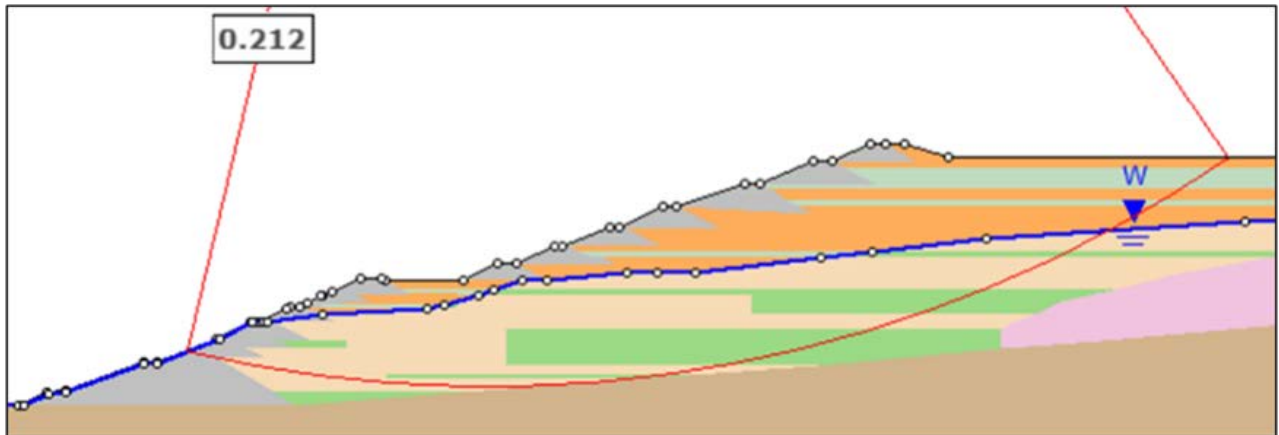


Figure 6: Slip Surface from Slide2 for post-liquefaction analysis

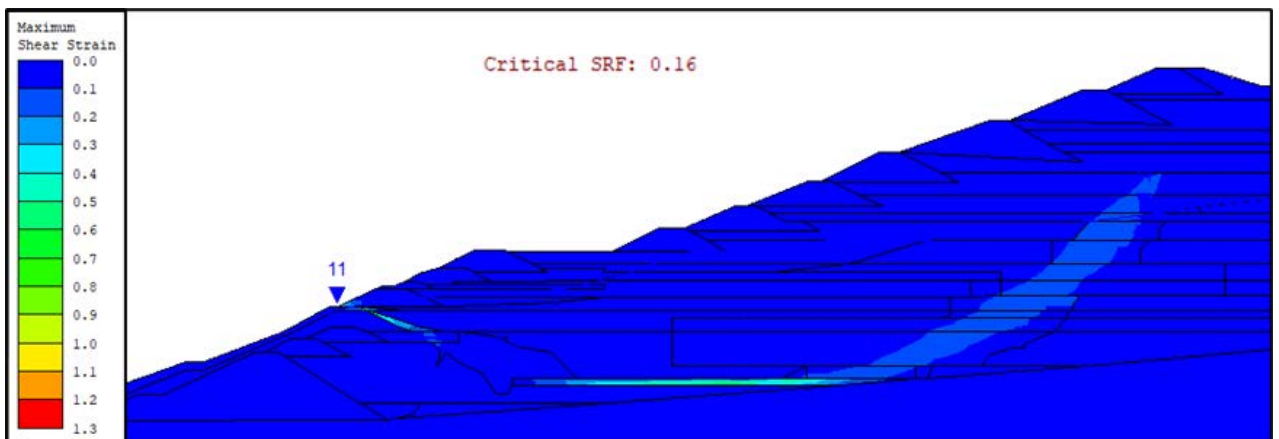


Figure 7: Slip Surface from RS2 for progressive failure analysis

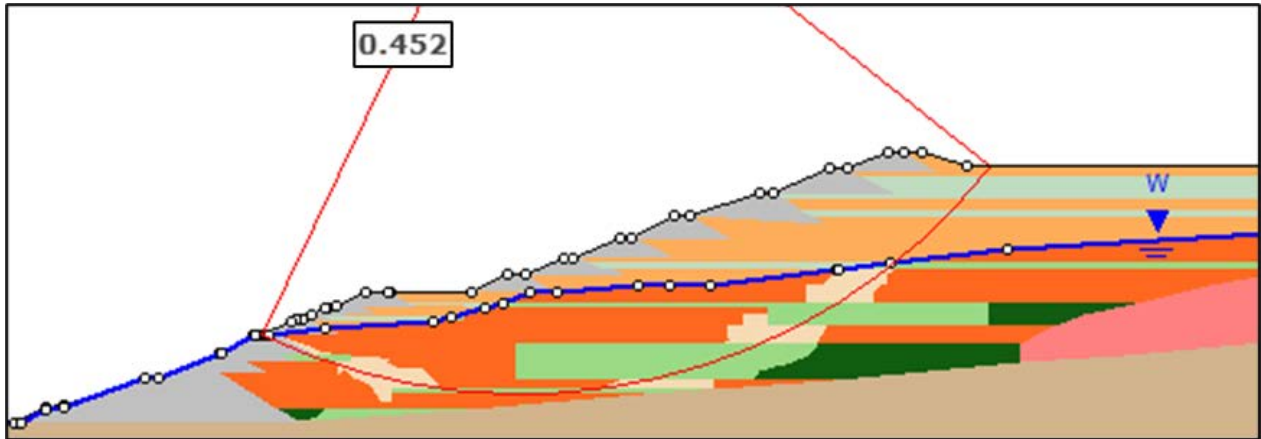


Figure 8: Slip surface from slide for progressive failure analysis

According to the above figures, a relatively smaller mass of tailings undergoes failure in a progressive failure analysis compared to the post-liquefaction analysis. This is compatible with the observed failure of the dam from the video footage of the failure, as well as in the image analysis done by the expert panel (Robertson et al., 2019). Figure 9 is a compilation of some photographs from the report that shows the possible initial failure area of the dam. The areas of lighter pink colour indicate larger displacements. The area of the largest displacement is the green shape near the bottom of the dam. This area corresponds with Section 3'–3' of the dam with most of the displacement produced in the second raise.

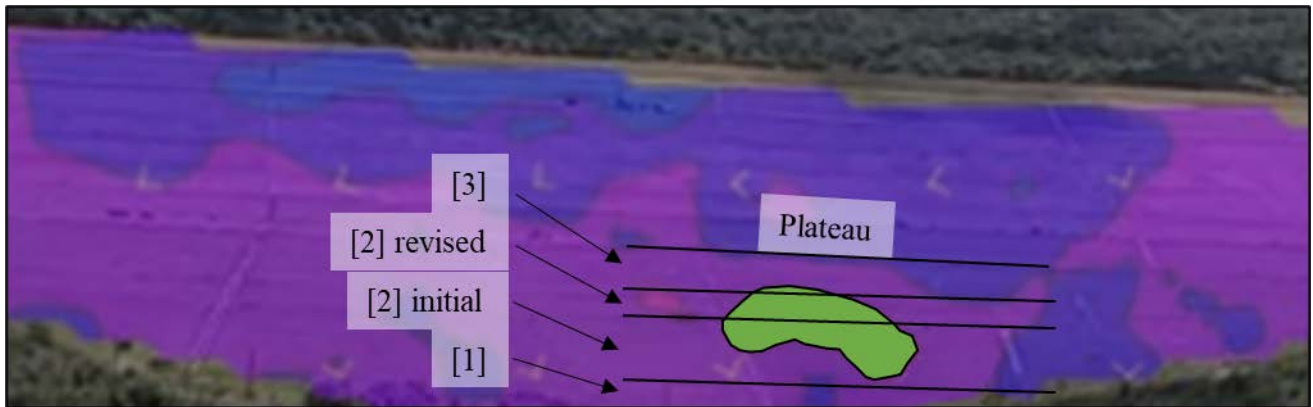


Figure 9: Compilation of photographs from the expert report (Robertson et al., 2019) potentially indicating the initial failure region

Conclusions

An energy method was introduced in this study for examining the susceptibility of soils to static liquefaction. This method has the advantage of being independent of stress path.

Multiple finite element and limit equilibrium models of the Feijão tailings dam were created: a triggering model where the saturated tailings were assigned their liquefaction triggering strength; a post-

liquefaction model where the saturated tailings were assigned their post-liquefaction strength; and then a progressive failure model. The energy method was used to determine sections of the tailings in the progressive failure model that would likely liquefy; these sections were then assigned $s_u(\text{liq})$, whereas the rest of the tailings were assigned $s_u(\text{yield})$. An iterative process was used to account for the phenomenon where soil liquefaction can trigger other nearby soils to liquefy.

Slip surfaces were attained for the finite element and limit equilibrium models, as well as strength reduction factors and factors of safety, respectively. The slip surfaces determined from the progressive failure analysis were consistent with field observations, and reasonably predicted failure of the tailings mass.

References

- Dief, H. 2000. Evaluating the liquefaction potential of soils by the energy method in the centrifuge. Doctoral thesis, Case Western Reserve University.
- Green, R. 2001. Energy-based evaluation and remediation of liquefiable soils. Doctoral thesis, Virginia Polytechnic Institute and State University.
- Griffiths, D.V. and P.A. Lane. 1999. Slope stability analysis by finite elements. *Géotechnique* 49(3): 387–403.
- Hill, R. 1958. A general theory of uniqueness and stability in elastic-plastic solids. *Journal of the Mechanics and Physics of Solids* 6: 236–249.
- Jefferies, M. and K. Been. 2016. *Soil Liquefaction: A Critical State Approach* (2nd ed.) Florida: Routledge Taylor & Francis Group.
- Kokusho, T. 2013. Liquefaction potential evaluations: energy-based method versus stress-based method. *Canadian Geotechnical Journal* 50(10): 1088–1099.
- Lade, P. 1992. Static instability and liquefaction of loose fine sandy slopes. *Journal of Geotechnical Engineering* 118(1): 51–71.
- Liang, L. 1995. Development of an energy method for evaluating the liquefaction potential of a soil deposit. Doctoral thesis, Case Western Reserve University.
- Morgenstern, R., S. Vick, C. Viotti and B. Watts. 2016. Fundão tailings dam review panel: report on the immediate causes of the failure of the Fundão dam.
- Robertson, P., L. de Melo, D. Williams and G.W. Wilson. 2019. Report of the expert panel on the technical causes of the failure of Feijão Dam 1.
- Sadrekarami, A. 2016. Static liquefaction analysis considering principal stress directions and anisotropy. *Geotechnical and Geological Engineering* 34(4): 1135–1154.

- Sadrekarami, A. 2020. Forewarning of static liquefaction landslides. *Journal of Geotechnical and Geoenvironmental Engineering* 146(9): 1–14.
- Silvis, F. and M.B. de Groot. 1995. Flow slides in The Netherlands: experience and engineering practice. *Canadian Geotechnical Journal* 32(6): 1086–1092.